Giulia Buttazzoni
Department of Engineering and Architecture
University of Trieste
34127 Trieste, Italy
gbuttazzoni@units.it

Elena Marongiu
Department of Electrical and Electronic Engineering
University of Cagliari
09123 Cagliari, Italy
e.marongiu10@studenti.unica.it

Fulvio Babich
Department of Engineering and Architecture
University of Trieste
34127 Trieste, Italy
babich@units.it

Alessandro Fanti
Department of Electrical and Electronic Engineering
University of Cagliari
09123 Cagliari, Italy
alessandro.fanti@unica.it

Francesca Vatta
Department of Engineering and Architecture
University of Trieste
34127 Trieste, Italy
vatta@units.it

Massimiliano Comisso
Department of Engineering and Architecture
University of Trieste
34127 Trieste, Italy
mcomisso@units.it

***Abstract*—Thanks to their versatility, smart antenna arrays are used in a wide variety of contexts, including, in particular, coastal monitoring. Within this framework, operating in multi-frequency modality might reveal a fundamental requirement. So, in this paper the problem of synthesis of multi-frequency antenna arrays is addressed. Precisely, a fixed grid array is considered, having an arbitrary but known geometry. The excitation vectors are optimized in such a way that the radiation patterns belong to a prescribed mask at certain assigned frequencies. Moreover, in order to have a simpler, cheaper and more efficient antenna, the phase-only synthesis is performed. In fact, thanks to this requirement, variable attenuators are not necessary and only phase-shifters are used in the feeding network. Numerical examples are provided, which validate the effectiveness of the method.**

***Index Terms*—antenna arrays, coastal monitoring, multi-frequency synthesis, phase-only control, smart antennas**

I. Introduction

The metrology of the sea involves social, economic and environmental aspects of our everyday lives. Thus, the research in the field of metrology for marine environment attracts the interest of national and international institutions, both from industries and governments, as well as from academia. Within this framework, real-time monitoring of the sea and in particular of the coasts is of great importance in many applications, ranging from the protection of coastal environment, to homeland security, from the monitoring of fishery to the detection of oil spills, just to name a few. This is why nowadays, the importance of coastal monitoring is universally recognized, so that many research programs have been proposed and funded worldwide during the last decades to achieve the so-called 'marine awareness' [1]–[6].

The proliferation of such projects highlights the broad consensus and the need for an integrated ocean observing system to promote a sustainable use of coastal resources by providing more and more information in scales of time and space [2]. Coastal management requirements can be both fast episodic events (such as oil spills) and slow cyclical processes (such as coastal erosion). It is evident that this range of information needs to reflect different spatial and temporal scales. In addition, they interest different end-users, for whom a successful coastal observing system requires continuous and easy methods of data archiving, extraction and distribution. Within this framework, satellite remote sensing represents a cost-effective, long-term and real-time acquisition tool to continuously monitor the coastal environments, so as to be able to predict future trends.

Of course, remote sensing requires a proper antenna system to acquire the necessary data. In this context, smart antenna arrays are recognized as a viable solution, thanks to the great versatility they provide [7]–[12]. In particular, multi-frequency antenna arrays offer some beneficial aspects in the coastal monitoring process [13] and ocean-observing satellite missions, in general [11]. So, in this paper a method of synthesis for multi-frequency smart antenna arrays for coastal monitoring is proposed. Precisely, given an antenna array, having an arbitrary number of elements, the excitation vectors are synthesized at a number of prescribed frequencies. Moreover, in order to simplify the feeding network and to

improve the efficiency of the antenna system, the phase-only synthesis is imposed. In particular, the amplitude of the excitations are optimized, but they are required to be constant for all the considered frequencies, while only the phases of the excitations are modified. Importantly, the proposed method is suitable for arrays of arbitrary (but fixed geometry) and can be used in real-case situations, since it allows to consider the mutual coupling between adjacent elements and, eventually, the influence of other components on the active element patterns of the array elements. The developed procedure of synthesis is based on the alternating projection approach, which is a deterministic iterative procedure for finding a point belonging to the intersection between two sets.

The remaining of this paper is organized as follows. The addressed problem is formulated in Section II, whereas Section III describes the developed procedure of synthesis. Numerical results are proposed in Section IV, which proves the effectiveness of the method. Finally, conclusions are summarized in Section V.

II. Problem Description

With reference to a Cartesian system $O(x, y, z)$, let consider an arbitrary antenna array composed by N radiating elements. Let $\bar{\mathbf{r}}_n = x_n\hat{\mathbf{i}} + y_n\hat{\mathbf{j}} + z_n\hat{\mathbf{k}}$ denote the position of the n-th element, being $\hat{\mathbf{i}}, \hat{\mathbf{j}}, \hat{\mathbf{k}}$ the unit vectors of the axes x, y, z, respectively. The far-field pattern of the array at the generic direction $\hat{\mathbf{r}} = \sin\theta\cos\phi\,\hat{\mathbf{i}} + \sin\theta\sin\phi\,\hat{\mathbf{j}} + \cos\theta\,\hat{\mathbf{k}}$, with θ and ϕ the polar and the azimuth angle, respectively, can be expressed as [14]:

$$F(\hat{\mathbf{r}}; f; \mathbf{a}) = \sum_{n=1}^{N} a_n\, p_n(\hat{\mathbf{r}}; f) \exp(jk\bar{\mathbf{r}}_n \cdot \hat{\mathbf{r}}), \tag{1}$$

where $f = c/\lambda$ is the frequency (being c the speed of light and λ the wavelength), $\mathbf{a} = [a_1, \ldots, a_N]$ is the vector of the (complex) excitations, j is the imaginary unit and $k = 2\pi/\lambda$ is the wave-number, $p_n(\hat{\mathbf{r}}; f)$ is the embedded element pattern of the n-th element in the direction $\hat{\mathbf{r}}$ at frequency f, i.e. the radiation pattern of the entire array when only the n-th element is excited and all the others are terminated on matched loads. It is worth noting that the radiation pattern in (1) takes into account the mutual coupling between the array elements, as well as the influence of the environment on the radiation performance of the entire structure.

Now, let consider a far-field pattern mask:

$$M = \{g(\hat{\mathbf{r}}) \in \mathbb{C} : M_{\text{low}}(\hat{\mathbf{r}}) \leq |g(\hat{\mathbf{r}})| \leq M_{\text{up}}(\hat{\mathbf{r}})\}, \tag{2}$$

where $M_{\text{low}}(\hat{\mathbf{r}}), M_{\text{up}}(\hat{\mathbf{r}})$ are two positive functions, representing the lower and upper bounds of the mask, respectively. Then, let consider a number S of desired frequencies $f_s, s = 1, \ldots, S$.

The problem addressed in this paper is that of finding S excitation vectors $\mathbf{a}_s = [a_{1s}, \ldots, a_{Ns}]$ such that:

$$F(\hat{\mathbf{r}}; f_s; \mathbf{a}_s) \in M, \qquad s = 1, \ldots, S; \tag{3}$$

$$|a_{n1}| = \cdots = |a_{nS}|, \qquad n = 1, \ldots, N. \tag{4}$$

Constraint (3) imposes that the far-field radiation pattern belongs to the mask at all the desired frequencies f_s, while constraint (4) imposes that the excitation amplitude of the n-th element be the same for all the S excitation vectors, in order to realize the so-called phase-only control.

III. Method of Synthesis

The developed synthesis procedure is based on the alternating projection approach [15], which is an iterative procedure for finding a point belonging to the intersection between two sets. So, first of all, the problem is formulated in terms of intersection finding problem.

In order to do so, the set $\mathbf{W}$ is introduced, whose elements are:

$$\tilde{\mathbf{w}} = \{\boldsymbol{\alpha}_1, \ldots, \boldsymbol{\alpha}_S, \kappa_1(\hat{\mathbf{r}}), \ldots, \kappa_S(\hat{\mathbf{r}})\}, \tag{5}$$

where $\boldsymbol{\alpha}_s = [\alpha_{1s}, \ldots, \alpha_{Ns}]$ are arbitrary (complex) vectors and $\kappa_s(\hat{\mathbf{r}})$ are arbitrary (complex) functions. Then, in $\mathbf{W}$ two subsets $\mathbf{U}$ and $\mathbf{V}$ are introduced, whose elements are defined as follows:

$$\tilde{\mathbf{u}} = \{\mathbf{u}_1, \ldots, \mathbf{u}_S, g_1(\hat{\mathbf{r}}), \ldots, g_S(\hat{\mathbf{r}}) : g_s(\hat{\mathbf{r}}) \in M, \\ |u_{n1}| = \cdots = |u_{nS}|, n = 1, \ldots, N,\ s = 1, \ldots, S\}, \tag{6}$$

$$\tilde{\mathbf{v}} = \{\mathbf{v}_1, \ldots, \mathbf{v}_S, F(\hat{\mathbf{r}}; f_1; \mathbf{v}_1), \ldots, F(\hat{\mathbf{r}}; f_S; \mathbf{v}_S)\}. \tag{7}$$

In other words, the elements of $\mathbf{W}$ are $2S$-tuples composed by S arbitrary vectors having N (complex) elements and S arbitrary complex scalar functions. Then, the elements of $\mathbf{U}$ are composed by S complex vectors, which satisfy constraint (4) and S scalar functions, which satisfy constraint (3). However, they have no relations with the antenna array under examination. On the other hand, the elements of $\mathbf{V}$ are composed by S arbitrary complex vectors and the S far-field patterns radiated by the array under examination at the S frequencies of interest. It is to be noted that the elements of $\mathbf{V}$ satisfy the array equation (1), but not the constraint of the problem.

So now, it is evident that any element belonging to both the sets $\mathbf{U}$ and $\mathbf{V}$ is a solution to the considered problem, which is formulated as an intersection finding problem, and can be solved by the alternating projection approach as described below.

First of all, in order to introduce the projector operators, the following squared distance between two elements $\tilde{\mathbf{w}}, \tilde{\mathbf{w}}' \in \mathbf{W}$ is defined as:

$$\rho^2(\tilde{\mathbf{w}}, \tilde{\mathbf{w}}') = \sum_{s=1}^{S} \left[\|\boldsymbol{\alpha}_s - \boldsymbol{\alpha}'_s\|_E^2 + \|\kappa_s(\hat{\mathbf{r}}) - \kappa'_s(\hat{\mathbf{r}})\|^2\right]. \tag{8}$$

In (8), $\|\boldsymbol{\alpha}\|_E$ represents the Euclidean norm of vector $\boldsymbol{\alpha}$ and $\|\kappa(\hat{\mathbf{r}})\|$ represents the mean-square norm of function $\kappa(\hat{\mathbf{r}})$. Once the distance has been defined, the projector of point $\tilde{\mathbf{w}}$ onto the set $\mathbf{X}(\subset \mathbf{W})$ can be defined as:

$$\mathcal{P}_{\mathbf{X}} : \mathbf{W} \to \mathbf{X}, \\ \tilde{\mathbf{w}} \mapsto \tilde{\mathbf{x}} = \arg\min_{\tilde{\mathbf{x}} \in \mathbf{X}} \rho(\tilde{\mathbf{w}}, \tilde{\mathbf{x}}). \tag{9}$$

This implies that the projector of a point $\tilde{\mathbf{w}}$ onto the set $\mathbf{X}$ is the operator which associates to $\tilde{\mathbf{w}}$ the point(s) $\tilde{\mathbf{x}}$ of $\mathbf{X}$ having the minimum distance from $\tilde{\mathbf{w}}$. Here, it is important to emphasize that, if the set $\mathbf{X}$ is closed such a point exists. If, in addition, $\mathbf{X}$ is also convex the projection is unique. But, if $\mathbf{X}$ is not convex, more than one point could exist, which satisfies the condition (9).

Now, once the projection operator has been defined, in order to find a point belonging to the intersection $\mathbf{U} \cap \mathbf{V}$, starting from a suitable point $\tilde{\mathbf{u}}_0 \in \mathbf{U}$, the following iterative procedure can be introduced:

$$\tilde{\mathbf{u}}_{n+1} = \mathcal{P}_{\mathbf{U}}[\mathcal{P}_{\mathbf{V}}(\tilde{\mathbf{u}}_n)], \qquad n = 0, 1, 2, \ldots \tag{10}$$

Thanks to the properties of the projector and of the distance, the sequence of distances from $\tilde{\mathbf{u}}_n$ to $\mathbf{V}$ is non-increasing, thus it converges to a point of $\mathbf{U}$ minimizing the distance from $\mathbf{V}$. Unfortunately, $\mathbf{U}$ is non-convex and the intersection may be empty, so the iteration is terminated when:

$$\rho(\tilde{\mathbf{u}}_n, \mathbf{V}) < \varepsilon \quad \text{or} \quad \frac{\rho(\tilde{\mathbf{u}}_{n-1}, \mathbf{V}) - \rho(\tilde{\mathbf{u}}_n, \mathbf{V})}{\rho(\tilde{\mathbf{u}}_n, \mathbf{V})} < \delta, \tag{11}$$

where ε and δ are two suitable thresholds.

The expressions of the projector operators $\mathcal{P}_{\mathbf{U}}$ and $\mathcal{P}_{\mathbf{V}}$ can be derived following, for example, the procedure developed in the appendix of [15] and are not shown here.

IV. Numerical Results

In this section two numerical examples are presented, which prove the effectiveness of the developed approach for the multi-frequency phase-only synthesis of smart antennas. Both the examples are implemented using Matlab on a commercial laptop equipped with an Intel(R) Core(TM) i7-12800H processor and 16 GB RAM. In both the examples the pattern cut at $\theta = \pi/2$ is considered, corresponding to the xy-plane, where $\hat{\mathbf{r}} = \cos\phi\ \hat{\mathbf{i}} + \sin\phi\ \hat{\mathbf{j}}$. Moreover, isotropic patterns are assumed for all the elements at all the considered frequencies, i.e., $p_n(\hat{\mathbf{r}}; f_s)$ for $n = 1, \ldots, N, s = 1, \ldots, S$. By doing so, the radiation patterns in (1) become array factors and only the dependency on ϕ is considered. In both the examples, as the starting point for the procedure in (10) the point $\tilde{\mathbf{u}}_0 \in U$ is chosen, which is composed by S null vectors and by S identical scalar functions, corresponding to $M_{\text{low}}(\hat{\mathbf{r}})$. The thresholds for the stop condition in (11) are set as $\varepsilon = \delta = 10^{-6}$. Then, in both the cases the problem is first solved for a single frequency value and the array factors are evaluated at the other desired frequencies with the optimized excitation vector. As it will be shown in Fig. 1 and Fig. 2, by doing so, only the array factor at the design frequency belongs to the mask, while a strong pattern distortion is obtained at the other frequencies, resulting in a violation of constraint (3). (It is worth to note that the single-frequency is performed both at the maximum and at the central desired frequency, and the pattern distortion occurs in both the cases.) This proves the necessity of having a synthesis procedure, which takes into account the multi-frequency design as an optimization requirement.

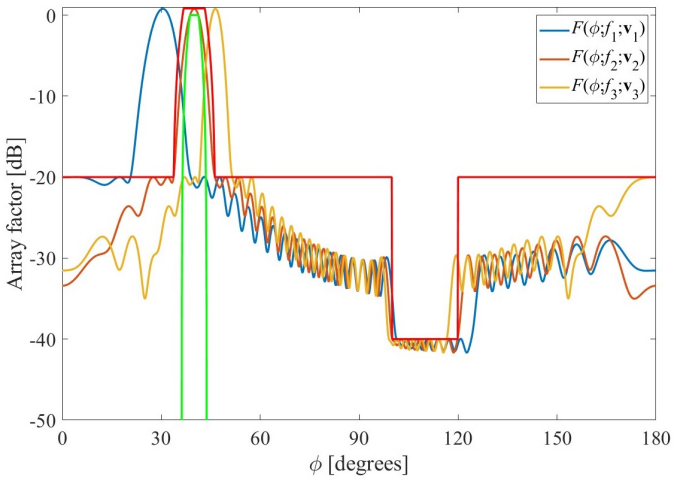

(a)

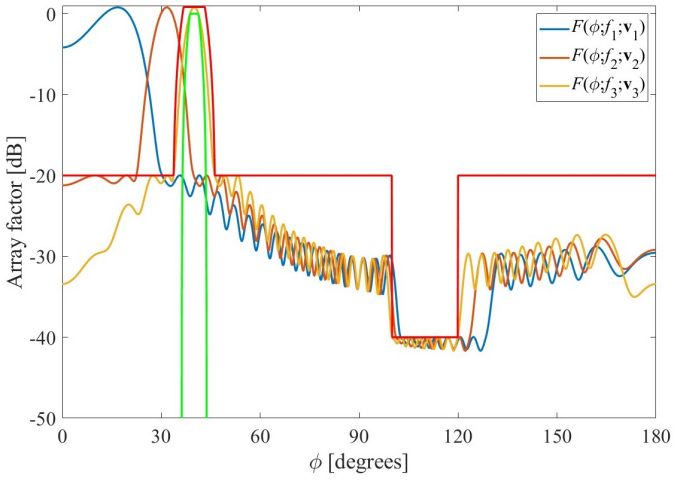

(b)

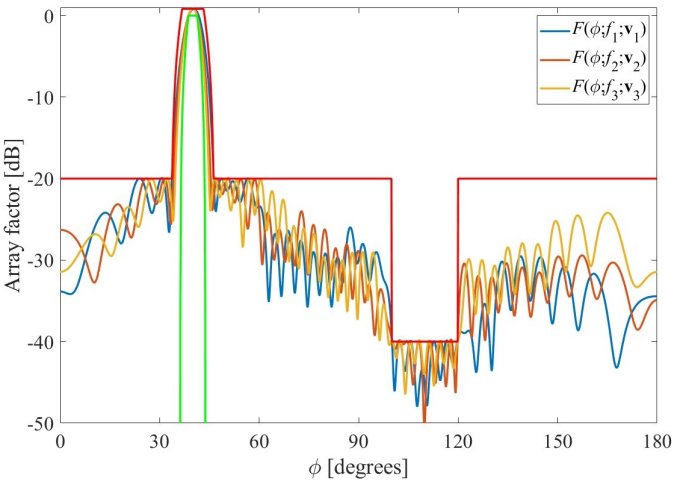

(c)

Fig. 1. Example 1: the $S = 3$ array factors radiated by the linear array with the synthesized excitation vectors. (a): single-frequency synthesis performed at $f = 0.9 f_{\max}$. (b): single-frequency synthesis performed at $f = f_{\max}$. (c): proposed multi-frequency approach.

A. Example 1: Linear Array

The first numerical example considers a uniform linear antenna array composed by $N = 40$ elements lying on the x-axis at the positions $x_n = nd$, where $d = \lambda_{\min}/2$ with $\lambda_{\min} = c/f_{\max}$. The following $S = 3$ frequencies are considered,

$$f_s = [1 - 0.1(S - s)]f_{\max}, \quad s = 1, \ldots, S. \tag{12}$$

Due to the symmetry of the antenna array, the synthesis is performed in the portion of the xy-plane having $\phi \in [0°, 180°]$. Finally, the lower and the upper bound of the mask are defined as piece-wise linear functions, which are represented as the green and the red line, respectively, in Fig.1. It is to be noted, that the mask also includes a wide null region in the interval $\phi \in [100°, 120°]$.

With the above data, the iterative procedure in (10) stops after 473 iterations (performed in less than 1 s of CPU time). According to the deveolped algorithm, being the final point $\tilde{\mathbf{u}}_{473} \in \mathbf{U}$, constraint (4) is rigorously satisfied. The element excitations are listed in Tab. I (for each element, the amplitude of the excitation is common for the S frequencies, which is provided in the second column, while the third, fourth and fifth columns provide the element phases corresponding to the different frequencies). On the other hand, constraint (4) is only approximated. However, Fig. 1(c) shows that the results are quite satisfactory. In particular, the maximum sidelobe level is -19.89 dB and the maximum null level is -39.71 dB.

B. Example 2: Circular Array

The second numerical example considers a uniform circular antenna array composed by $N = 200$ elements lying on the xy-plane at the positions $x_n = R\cos(2n\pi/N), y_n = R\sin(2n\pi/N)$, where $R = 15.9\lambda_{\min}$, with $\lambda_{\min} = c/f_{\max}$. Then, $S = 7$ frequencies are considered, which are still chosen according to (12). The synthesis is performed on the entire xy-plane ($\phi \in [0°, 360°]$).

With the above data, the iterative procedure in (10) stops after 720 iterations (approximately 36 s of CPU time). The array factors are shown in Fig.2, along with the lower and the upper bound of the mask. As it can be seen, also in this second example, constraint (3) is very well approximated (the maximum sidelobe level is -14.96 dB), while, of course, constraint (4) is rigorously satisfied (due to reasons of space, the element excitations are not reported for this example, having a high number of elements and considered frequencies).

V. Conclusion

An innovative algorithm for the synthesis of multi-frequency smart antenna arrays has been proposed for the coastal monitoring. The algorithm is suitable for arrays of arbitrary geometry. It allows to optimize the array element excitations, in such a way that the radiation pattern belongs to an assigned mask at all the desired frequencies. Interestingly, each array element has the same amplitude, and only its phase is modified at the different frequencies. This is the phase-only control, which allows to simplify the feeding network and to improve

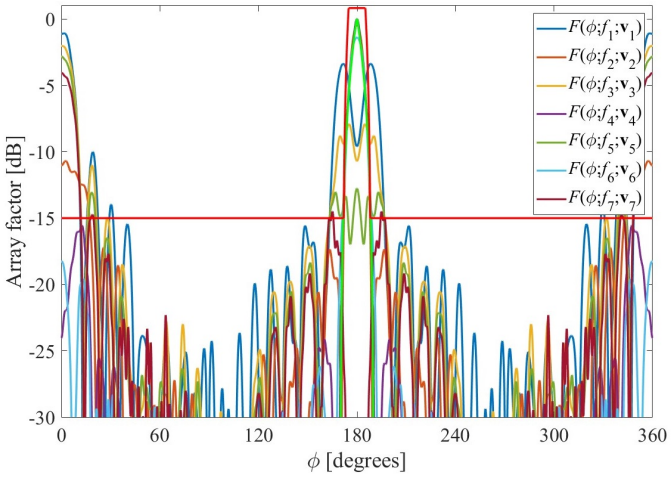

(a)

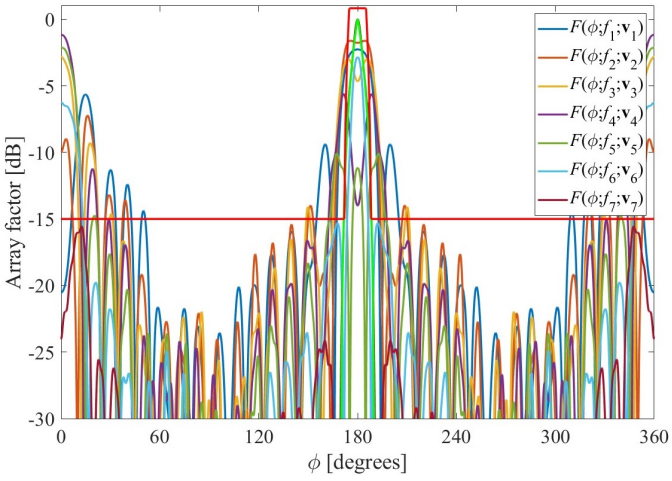

(b)

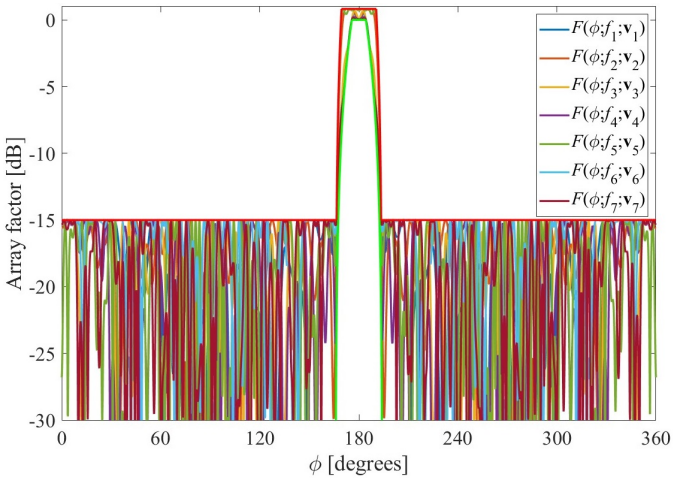

(c)

Fig. 2. Example 2: the $S = 7$ array factors radiated by the circular array with the synthesized excitation vectors. (a): single-frequency synthesis performed at $f = 0.7f_{\max}$. (b): single-frequency synthesis performed at $f = f_{\max}$. (c): proposed multi-frequency approach.

TABLE I
EXAMPLE 1: SYNTHESIZED ELEMENT EXCITATIONS

n	$\lvert u_{ns}\rvert$	$\angle u_{n1}$	$\angle u_{n2}$	$\angle u_{n3}$
1	0.034	-1.6	-5.1	-12.4
2	0.042	-120.8	-126.4	-138.6
3	0.029	120.8	110.1	88.1
4	0.028	6.3	-20.0	-43.3
5	0.025	-79.4	-135.8	174.8
6	0.027	179.9	110.6	28.6
7	0.030	58.3	-15.8	-106.8
8	0.031	-46.7	-145.3	108.9
9	0.032	-161.6	81.6	-25.5
10	0.032	77.2	-44.7	-161.3
11	0.031	-32.1	-164.8	60.7
12	0.031	-138.8	75.2	-74.5
13	0.034	113.6	-47.2	146.8
14	0.035	3.6	-172.7	8.4
15	0.035	-101.8	65.2	-130.0
16	0.037	153.5	-59.0	91.5
17	0.037	41.3	178.0	-46.8
18	0.038	-73.7	50.6	176.6
19	0.037	177.5	-76.5	39.4
20	0.036	65.9	160.7	-98.7
21	0.035	-46.8	38.9	124.9
22	0.034	-154.3	-81.0	-14.8
23	0.034	97.1	152.6	-153.1
24	0.033	-13.5	27.0	69.0
25	0.031	-121.8	-97.6	-71.1
26	0.029	130.0	137.6	152.0
27	0.029	21.5	14.4	14.0
28	0.027	-91.3	-113.7	-123.0
29	0.024	158.0	122.1	100.9
30	0.023	49.8	0.9	-35.3
31	0.020	-61.8	-114.2	-175.1
32	0.020	-173.3	125.2	49.7
33	0.017	77.6	-6.7	-89.0
34	0.015	-28.1	-138.1	126.8
35	0.012	-145.0	88.3	-5.2
36	0.011	116.2	-25.8	-157.0
37	0.010	5.5	-138.4	67.1
38	0.010	-110.7	83.7	-62.6
39	0.015	128.2	-36.5	159.5
40	0.010	3.2	-165.9	32.5

the overall antenna efficiency. Of course, this is paid for by a reduction of the degrees of freedom of the problem. However, two numerical examples are provided, which proves the effectiveness of the developed algorithm in synthesizing multi-frequency smart antenna arrays by phase-only control.

In the future, in order to increase the versatility of the proposed approach three possible developments will be explored. First of all, different masks will be defined at the different considered frequencies. By doing so, it will be possible to realize the frequency notching, for example. Second, a constraint on the optimized amplitudes of the excitations will be included in the synthesis process, which is particularly interesting in those applications where the power consumption is a critical issue. Thirdly, in order to improve the achievable performance, the positions of the array elements will also be optimized, in such a way as to increase the degrees of freedom of the problem. Finally, it will be very interesting to test the algorithm in practical situations, in order to assess its ability to distinguish different targets according to the adopted frequency and to compare its performance with other state-of-the-art methods.

REFERENCES

[1] S. Phinn, P. Scarth, C. Roelfsema, B. Dennison, A. Dekker, and V. Brando, "Approaches for monitoring benthic and water column biophysical properties in australian coastal environments," in *IEEE Int. Geoscience Remote Sens. Symp. (IGARSS)*, July 2001, pp. 616–618.

[2] P. Siri, B. Heneman, S. Schuchat, S. Semans, and B. Smyth, "Developing observing system products for coastal management: applying surface current monitoring to coastal ocean management," in *Europe Oceans 2005*, June 2005, pp. 1199–1204 Vol. 2.

[3] M. Heron, "The Australian Coastal Ocean radar Network facility," in *Canadian Conf. Elect. Comput. Eng.*, May 2009, pp. 23–26.

[4] K. Laws, J. Vesecky, and J. Paduan, "Predicting the capabilities of ship monitoring by HF radar in coastal regions," in *OCEANS'11 MTS/IEEE KONA*, Sept. 2011, pp. 1–5.

[5] M. de Martino, S. Dellepiane, L. Gemme, G. Moser, S. B. Serpico, M. Toma, C. Degano, A. Loiaconi, I. Mainenti, L. A. Cusati, and A. Pedroncini, "The SEAGOSS project: Monitoring coastal seawater in Italy by remote sensing data," in *IEEE Int. Geoscience Remote Sens. Symp. (IGARSS)*, July 2014, pp. 4454–4457.

[6] R. Flagg, T. J. Owca, L. M. Marshall, A. Snauffer, J. Bedard, and M. Hoeberechts, "Cabled community observatories for coastal monitoring - developing priorities and comparing results," in *Global Oceans 2020: Singapore – U.S. Gulf Coast*, Oct. 2020, pp. 1–8.

[7] D. C. Law, S. A. McLaughlin, D. A. Merritt, and S. A. Pezoa, "Electronically-stabilized 915 MHz phased array antenna for ship-borne atmospheric wind profiling," in *IEEE Int. Symp. Phased Array Syst. Technol.*, May 2000, pp. 77–80.

[8] M. V. Ivashina, O. Iupikov, R. Maaskant, W. A. V. Cappellen, and T. Oosterloo, "An optimal beamforming strategy for wide-field surveys with phased-array-fed reflector antennas," *IEEE Transactions on Antennas and Propagation*, vol. 59, pp. 1864–1875, 6 2011.

[9] K. F. Warnick, M. V. Ivashina, S. J. Wijnholds, and R. Maaskant, "Polarimetry with phased array antennas: Theoretical framework and definitions," *IEEE Trans. Antennas Prop.*, vol. 60, pp. 184–196, Jan. 2012.

[10] C. Cappellin, K. Pontoppidan, P. H. Nielsen, N. Skou, S. S. Sobjarg, M. Ivashina, O. Iupikov, A. Ihle, D. Hartmann, and K. V. T. Klooster, "Novel multi-beam radiometers for accurate ocean surveillance," in *Eur. Conf. Antennas Prop. (EUCAP)*, Apr. 2014, pp. 3531–3535.

[11] O. A. Iupikov, M. V. Ivashina, C. Cappellin, and N. Skou, "Digital-beamforming array antenna technologies for future ocean-observing satellite missions," in *IEEE Int. Symp. Antennas Prop. (APSURSI)*, June 2016, pp. 1377–1378.

[12] M. H. Golbon-Haghighi, M. Mirmozafari, H. Saeidi-Manesh, and G. Zhang, "Design of a cylindrical crossed dipole phased array antenna for weather surveillance radars," *IEEE Open J. Antennas Prop.*, vol. 2, pp. 402–411, Feb. 2021.

[13] J. F. Vesecky, K. Laws, and J. D. Paduan, "Monitoring of coastal vessels using surface wave hf radars: Multiple frequency, multiple site and multiple antenna considerations," in *IEEE Int. Geoscience Remote Sens. Symp. (IGARSS)*, July 2008, pp. 405–408.

[14] G. Buttazzoni, F. Babich, S. Pastore, F. Vatta, and M. Comisso, "Gaussian approach for the synthesis of periodic and aperiodic antenna arrays: Method review and design guidelines," *Sensors*, vol. 21, no. 7, p. 2343, Mar. 2021.

[15] R. Vescovo, "Reconfigurability and beam scanning with phase-only control for antenna arrays," *IEEE Trans. Antennas Propag.*, vol. 56, pp. 1555–1565, June 2008.